The Purcell Effect of Silver Nanoshell on the Fluorescence of Nanoparticles

Wallace C.H. Choy (1*), X.W. Chen (1,2), S.L. He (2), P.C. Chui
1 : Department of Electrical and Electronic Engineering, University of Hong Kong, Pokfulam Road, Hong Kong, China. *Corresponding author: chchoy@eee.hku.hk
2 : Centre for Optical and Electromagnetic Research, Zhejiang University; Joint Research Centre of Photonics of the Royal Institute of Technology (Sweden) and Zhejiang University, Zhijingang campus, Hangzhou 310058, China.

Abstract: *The Purcell effect on the spontaneously emission rate and fluorescence efficiency of nanoparticles with and without a silver nanoshell will be investigated which are important for nanoparticle applications in biomedical diagnostics, information storage and optoelectronics*

Introduction

Fluorescent nanomaterials, including organic and metallorganic dye molecules, fluorescent proteins, II-VI and III-V compound semiconductor nanoparticles, polymer/dye-based nanoparticles and silica/dye hybrid particles, have been the subject of intensive research in recent years for their vast applications ranging from biomedical therapeutics and diagnostics to information storage and optoelectronics. A wide range of physical and chemical methods has been developed for the synthesis of nanoparticles and nanoscale core-shell structures with controllable core radius and shell thicknesses [10,11]. For fluorescence based applications, fluorescence efficiency, i.e. the external quantum efficiency (η_{ext}) of the emitter, is an important issue. Due to the existence of pronounced nonradiative decay of excitons in the nanoscale structure, low η_{ext} is an often-observed feature. Most of the strategies so far employed aim to reduce the nonradiative decay rate [12-14] for improving the fluorescence efficiency. The direct and effective approach to improve η_{ext} is to increase radiative decay rate[15] and the out-coupling efficiency since η_{ext} is the product of internal quantum efficiency and the outcoupling efficiency. The enhancement of radiative decay rate results in the Purcell enhancement of the internal quantum yield [16,17]. However, there are few studies on increasing the radiative decay rate and out-coupling efficiency simultaneously in core-shell nanoparticles to enhance the fluorescence efficiency. Here, we will address this issue through a rigorous theoretical study on the spontaneous emission (SE) rate and the out-coupling efficiency of emitters in nanoscale structure. The study can provide a better physical understanding and optimal design of the nano-structure to achieve high-efficiency fluorescence.

Theoretical model

The structure and parameters of a multilayered sphere are displayed on Fig. 1. An emitting shell is sandwiched between two stacks of shells, i.e., P outer shells and Q inner shells. The relative permittivity and the boundary of the ith shell are denoted as ε_i (i = –Q,...,P) and r_{i+1} (i = –Q,..., P-1), respectively. The emitting medium and the outermost layer is assumed to be non-absorbing at the emitting wavelength. The quantum emitter can be modeled as incoherent classical electric dipoles. The SE of the emitter can be characterized by using the averaged total radiation power F and the power radiated to farfield U (normalized by the total radiation power of an electric dipole in infinite medium) of the dipoles in the spherically multilayered structure. As a consequence of Fermi's golden rule, the radiative decay rate is optical-environment-dependent as the radiative decay rate is optical-environment-dependent as [17,28] $\Gamma_r^s = F \cdot \Gamma_r^0$ where Γ_r^0 and Γ_r^s are the exciton radiative decay rate in free space and spherically multilayered media, respectively. The averaged total radiation power F, also called as the Purcell factor, can be considered as a normalized SE rate. The change of radiative decay rate will result in the change of the internal quantum efficiency since the radiative and non-radiative recombinations are competing processes. Assuming that the non-radiative decay rate in the spherically multilayered structure is Γ_{nr}, the internal quantum efficiency in the spherically multilayered media η_q^s is modified as

$$\eta_q^s \equiv \frac{\Gamma_r^s}{\Gamma_r^s + \Gamma_{nr}} = \frac{F}{F\eta_q^0 + \left(1-\eta_q^0\right)} \cdot \eta_q^0 \qquad (1)$$

where η_q^0 is the initial internal quantum efficiency when F=1. η_{ext} is given by

$$\eta_{ext} \equiv \eta_q^s \cdot \frac{U}{F} = \frac{U}{F\eta_q^0 + \left(1 - \eta_q^0\right)} \cdot \eta_q^0 \qquad (2).$$

In the presence of ultra-thin metallic shells, nonlocal effect due to excitations of longitudinal plasmon modes may come into play [22-24]. Then an additional boundary condition is required to characterize this effect [22-24] in determining F and U. We find that the nonlocal effect is prominent for silver shells thinner than 20 nm. The scheme for

calculating F here is general regardless of the permittivity of the other shells, while the scheme used in ref. [27] depends on the material of the other shells and becomes increasingly complicated when the number of lossy shells increases.
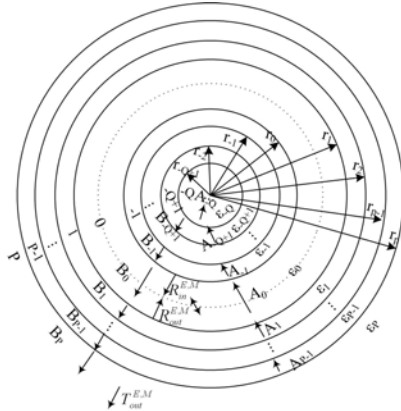

Fig.1 Geometry and parameters of a spherically multilayered structure. $R_{out,l}^{E/M}$, $R_{in,l}^{E/M}$ and $T_{out,l}^{E/M}$ are the total reflection coefficient from the outer shells, the total reflection coefficient from the inner shells and the total transmission coefficient of TE/TM polarization, respectively.

Result and Discussion

The dependences of the fluorescence efficiencies on the structural parameters are investigated for two initial internal quantum yields, i.e. $\eta_q^0 = 0.25$ and $\eta_q^0 = 0.75$. In the calculation, the refractive index of the nanoparticle (NP) is set to be 2.0 over the wavelength of interest. The dielectric function of bulk silver [32] is used in the calculation.

A. SE in a bare NP

SE properties of the emitters in a bare spherical NP with a radius r is studied and discussed in this subsection. Fig. 2(a) plots the wavelength dependence of the normalized SE rate of emitters located at the center of the NP with a radius of 20nm. One sees that the SE rate is nearly one tenth of the SE rate in free space and decreases gradually as the wavelength increases. The size dependence of the normalized SE rate at the wavelength of 500nm is shown in Fig. 2(b) as the solid line with filled squares. The SE rate decreases as the radius of the NP decreases. As shown in Fig. 2(b), due to the low SE rate (F), η_{ext} are much smaller than their initial quantum yields according to Eq. (2) where U equals F in the case of a bare NP. The degradation of η_{ext} for $\eta_q^0 = 0.25$ is more pronounced than that for $\eta_q^0 = 0.75$. This is because the ratio of radiative decay rate to nonradiative decay rate for $\eta_q^0 = 0.25$ drops faster as F decreases. Consequently, a bare NP usually shows inefficient fluorescence.

B. SE in the nanoparticle with a silver nanoshell

The SE rate can be greatly enhanced when the NP is encapsulated with a silver nanoshell due to the resonant excitation of surface plasmons. Unlike the previous case of a bare NP where U equals F, U is smaller than F in the present case since a considerable part of power is absorbed in the silver shell. Thus both F and U should be calculated for characterizing the SE properties. Here the thickness effect of the silver shell on the SE properties is studied for the silver encapsulated NP with various shell thickness s and a fixed core radius r of 30nm as shown in Fig. 3(a). Firstly, the spectrum of the SE rate shows a resonant structure and the SE rate at the resonant wavelength is several orders of magnitude larger than the SE rate in a bare NP due to the resonant excitation of surface plasmons.

The large increment of the SE rate will result in a great enhancement of the internal quantum efficiency due to the Purcell enhancement according to Eq. (1). Secondly, the resonant wavelength of the spectrum of the SE rate shows a blue shift as s increases. The results show that the peak value of the normalized SE rate (hereafter named "the peak SE rate") is reduced as s increases. To understand the reduction of the peak SE rate, we define an effective radius as $R = 2\pi r/\lambda_r$, where λ_r is the resonant wavelength, to characterize the strength of surface plasmon effects. The surface plasmon effect decreases exponentially as R increases. The inset of Fig. 3(a) shows the dependence of the effective radius on the shell thickness. It can be observed that the effective radius firstly increases as s increases. Thus in Fig. 3(a) the peak SE rate is reduced and the resonant spectrum broadens as s increases from 5nm to 30nm. Fig. 3(b) shows the dependence of the fluorescence efficiency at the resonant wavelength on the shell thickness. As compared with Fig. 2(b) for a bare NP, the fluorescence efficiency of the NP encapsulated with a suitable thickness of silver shell is much larger. Moreover, the fluorescence efficiency for the core-shell structure with $r = 30$nm and $s = 25$nm is much larger than the initial internal quantum efficiency. This is due to a combination of the Purcell enhancement of the internal quantum yield and a high out-coupling efficiency. From Fig. 3 (a) and 3(b), one sees that for the NP with ultra-thin silver shell although the SE rate is very large the fluorescence efficiency is still low since the out-coupling efficiency U/F is small, i.e. most of the emitted power is absorbed in the silver shell. As shown in Fig. 3(b), η_{ext} generally increases as s increases from 5nm to 25nm. As s further increases fluorescence decreases gradually since the absorption loss in the Ag shell increases again. Consequently, from Fig. 3(a) and 3(b), one sees that the fluorescence efficiency can be maximized through

simultaneously achieving a large Purcell enhancement and high out-coupling efficiency by carefully designing the Ag thickness.

Conclusions

In this paper, we have formulated a general approach for calculating the SE rate and η_{ext} of the emitters in a spherically multilayered structure with arbitrary permittivity. In the presence of silver nano-shell, nonlocal effect has been taken into account. By using the method, the SE rates and fluorescence efficiencies of the emitters in a bare NP and the NP with a silver nanoshell are investigated. The SE rate in a bare NP is only one tenth of the SE rate in free space and consequently the fluorescence is usually inefficient. The SE rate can be enhanced by orders of magnitude through encapsulating the NP with a silver nanoshell due to the resonant excitation of the surface plasmon. The spontaneous emission properties of the emitters in the NP with various thickness of silver nanoshell are studied. Through a proper design of the core-shell layer structure, highly efficient fluorescence can be achieved as a result of the combination of the large Purcell enhancement of quantum yield and a high outcoupling efficiency.

References

1. S.J. Oldenburg, R.D. Averitt, S.L. Westcott and N.J. Halas, "Nanoengineering of optical resonances," Chem. Phys. Lett. 288, 243 (1998).
2. C. Graf, A. van Blaaderen, "Metallodielectric colloidal core-shell particles for photonic applications," Langmuir 18, 524 (2002).
3. M.A. Hines and P. Guyot-Sionest, "Synthesis and characterization of strong luminescing ZnS-capped CdSe nanocrystals," J. Phys. Chem. 100, 468 (1996).
4. S. Haubold, M. Haase, A. Kornowski and H. Weller, "Strongly luminescent InP/ZnS core-shell nanoparticles," Chemphyschem, 2, 331 (2001).
5. N. Gaponik, D.V. Talapin, A.L. Rogach, K. Hoppe, E.V. Shevchenko, A. Kornowski, A. Eychmuller and H. Weller, "Thiol-Capping of CdTe nanocrystals:an alternative to organometallic synthetic routes," J. Phys. Chem. B 106, 7177 (2002).
6. J.R. Lakowicz, "Radiative Decay Engineering: Biophysical and Biomedical Applications," Anal.Biochem. 298, 1 (2001).
7. E. M. Purcell, "Spontaneous emission probabilities at radio frequencies," Phys. Rev., 69, 681 (1946).
8. W. Lukosz, ''Theory of optical-environment-dependent spontaneous emission rates for emitters in thin layers,''Phys. Rev. B 22, 3030 (1980).
9. K. Neyts, "Simulation of light emission from thin-film microcavities," J. Opt. Soc. Am. A 15, 962 (1998).
10. A.R. Melnyk, M.J. Harrison,"Theory of optical excitation of plasmons in metals," Phys. Rev. B 2, 835 (1970).
11. P.T. Leung, "Decay of molecules at spherical surfaces: nonlocal effects," Phys. Rev. B 42 7622 (1990).
12. A. Pack, M. Hietschold and R. Wannemacher, "Failure of local Mie theory: optical spectra of colloidal aggregates," Optics Comm. 194, 277 (2001).
13. A. Moroz, "A recursive transfer-matrix solution for a dipole radiating inside and outside a stratified sphere," Anna. Phys. 315, 352 (2005).
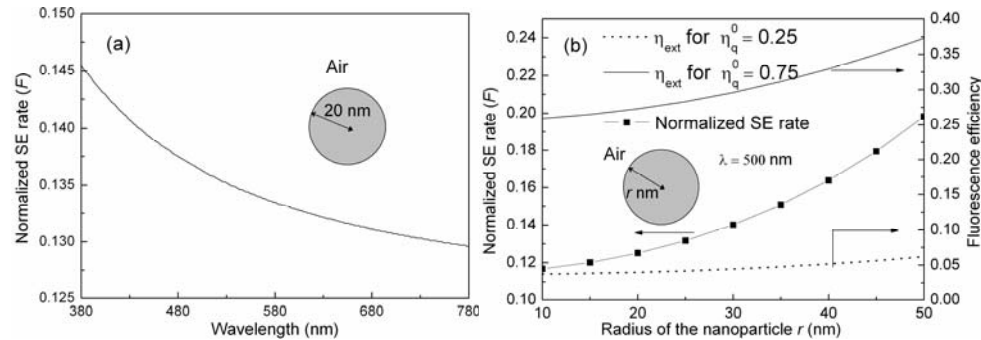14. E. D, Palik, Handbook of Optical Constants of Solids (Academic press, Boston, 1985)

Fig. 2(a) Wavelength dependence of the normalized SE rate for a fixed nanoparticle r = 20nm (b) Variance of the normalized SE rate and the fluorescence efficiency for $\eta_a^0 = 0.25$ and $\eta_a^0 = 0.75$ with the increase of the size of the nanoparticle at the wavelength of 500nm.
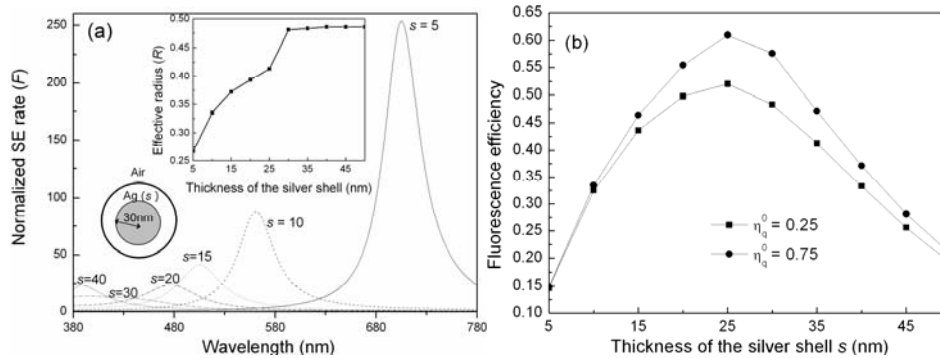

Fig. 3 (a) Wavelength dependence of the normalized SE rate in silver encapsulated nanoparticles of various Ag shell thicknesses s (nm) and fixed core radius; inset shows the variance of the effective radius with the increase of the shell thickness. (b) Variance of the fluorescence efficiency with the increase of Ag shell thickness and fixed core radius.